Inorganic Chemistry
Article

Inorg. Chem. **2010**, *49*, 3857–3865 **3857**
DOI: 10.1021/ic902549b

Luminescent Low-Valent Rhenium Complexes with 1,2-Bis(dialkylphosphino)ethane Ligands. Synthesis and X-ray Crystallographic, Electrochemical, and Spectroscopic Characterization

Stephania J. Messersmith, Kristin Kirschbaum, and Jon R. Kirchhoff*

Department of Chemistry, The University of Toledo, Toledo, Ohio 43606

Received December 29, 2009

A series of low-valent rhenium phosphine complexes with the general formula $[Re(dmpe)_{3-x}(depe)_x]^{2+/+}$ ($x = 0-3$), where dmpe is 1,2-bis(dimethylphosphino)ethane and depe is 1,2-bis(diethylphosphino)ethane, were synthesized and characterized. The reaction of $[Re(benzil)(PPh_3)Cl_3]$ with the appropriate phosphine yielded the homoleptic tris complexes $[Re(dmpe)_3]^+$ and $[Re(depe)_3]^{2+}$, while the mixed-ligand complexes $[Re(dmpe)_2(depe)]^+$ and $[Re(dmpe)(depe)_2]^{2+}$ were prepared from $[Re(dmpe)_2Cl_2]^+$ and $[Re(depe)_2Cl_2]^+$, respectively. The oxidation state of the final product strongly depends on the donating properties of the ligand. Each complex, however, exhibits a diffusion-controlled, reversible one-electron transfer between Re^{I} and Re^{II} with formal reduction potentials, $E^{\circ\prime}$, ranging from -0.09 to -0.28 V versus a ferrocene external standard. Subsequent oxidation to Re^{III} was found to be chemically irreversible. UV−vis and luminescence spectroelectrochemical techniques were used to study the spectral properties of the Re^{I} and Re^{II} forms. The Re^{II} complexes are red in color and exhibit absorption features from 350 to 600 nm; the lowest-energy transition was assigned as a $\sigma(P)$ to $d\pi(Re)$ ligand-to-metal charge-transfer (LMCT) transition. Excitation into the lowest-energy absorption band revealed rare examples of luminescent ($\Phi \approx 0.07$) LMCT excited states from d^5 transition-metal complexes in a room temperature solution. Structural characterization of salts of both oxidation states of $[Re(dmpe)_2(depe)]^{2+/+}$ was also performed.

Introduction

Luminescent transition-metal complexes have been investigated for many applications since the first report of luminescence from $[Ru(bpy)_3]^{2+}$,[1] which was subsequently shown to act as a photosensitizer for the photoinduced generation of H_2 and O_2 from H_2O.[2] Numerous applications as diverse as photocatalysts in energy conversion schemes,[3] precursors for supramolecular photocatalysts,[4] molecular probes for biomolecules,[5] nonlinear optical materials,[6] molecular wires,[7] and transducers in analytical sensors[8] have been proposed and demonstrated.

*To whom correspondence should be addressed. E-mail: jon.kirchhoff@utoledo.edu. Phone: (419) 530-1515. Fax: (419) 530-4033.

(1) Paris, J. P.; Brandt, W. W. *J. Am. Chem. Soc.* **1959**, *81*, 5001–5002.
(2) (a) Lehn, J.-M.; Sauvage, J.-P.; Ziessel, R. *Nouv. J. Chim.* **1980**, *4*, 355–358. (b) Kirch, K.; Lehn, J.-M.; Sauvage, J.-P. *Helv. Chim. Acta* **1979**, *62*, 1345–1384.
(3) (a) Esswein, M. J.; Nocera, D. G. *Chem. Rev.* **2007**, *107*, 4022–4047. (b) Garcia, C. G.; deLima, J. F.; Iha, N. Y. M. *Coord. Chem. Rev.* **2000**, *196*, 219. (c) Kalyanasundaram, K.; Gratzel, M. *Coord. Chem. Rev.* **1998**, *177*, 347–414. (d) Connolly, J. S. Solar Photochemistry. In *Alternative Fuels and the Environment*; Sterrett, F. S., Ed.; Lewis Publishers: Boca Raton, FL, 1995; Chapter 7.
(4) (a) Rangan, K.; Arachchige, S. M.; Brown, J. R.; Brewer, K. J. *Energy Environ. Sci.* **2009**, *2*, 410–419. (b) Sato, S.; Koike, K.; Inoue, H.; Ishitani, O. *Photochem. Photobiol. Sci.* **2007**, *8*, 454–461. (c) Balzani, V.; Ceroni, P.; Juris, A.; Venturi, M.; Campagna, S.; Puntoriero, F.; Serroni, S. *Coord. Chem. Rev.* **2001**, *219*, 545–572. (d) Armaroli, N. *Chem. Soc. Rev.* **2001**, *30*, 113–124. (e) Toma, H. E.; Araki, K. *Coord. Chem. Rev.* **2000**, *196*, 307–329. (f) Balzani, V.; Juris, A.; Venturi, M.; Campagna, S.; Serroni, S. *Chem. Rev.* **1996**, *96*, 759–833. (g) Sauvage, J. P.; Collin, J. P.; Chambron, J. C.; Guillerez, S.; Coudret, C.; Balzani, V.; Barigelletti, F.; DeCola, L.; Flamigni, L. *Chem. Rev.* **1994**, *94*, 993–1019.
(5) (a) Erkkila, K. E.; Odom, D. T.; Barton, J. K. *Chem. Rev.* **1999**, *99*, 2777–2795. (b) Yam, V. W. W.; Lo, K. K. W. *Coord. Chem. Rev.* **1999**, *184*, 157–240. (c) Stochel, G.; Wanat, A.; Kulis, E.; Stasicka, Z. *Coord. Chem. Rev.* **1998**, *171*, 203–220. (d) Stemp, E. D. A.; Barton, J. K. *Met. Ions Biol. Syst.* **1996**, *33*, 325–365. (e) Arkin, M. R.; Jenkins, Y.; Murphy, C. J.; Turro, N. J.; Barton, J. K. *Mech. Bioinorg. Chem.* **1995**, *246*, 449–469. (f) Gupta, N.; Grover, N.; Neyhart, G. A.; Liang, W.; Singh, P.; Thorp, H. H. *Angew. Chem., Int. Ed. Engl.* **1992**, *31*, 1048–1050. (g) Wuttke, D. S.; Bjerrum, M. J.; Winkler, J. R.; Gray, H. B. *Science* **1992**, *256*, 1007–1009.
(6) (a) Kar, S.; Miller, T. A.; Chakraborty, S.; Sarkar, B.; Pradhan, B.; Sinha, R. K.; Kundu, T.; Ward, M. D.; Lahiri, G. K. *Dalton Trans.* **2003**, 2591–2596. (b) Yam, V. W. W.; Lo, K. K. W.; Wong, K. M. C. *J. Organomet. Chem.* **1999**, *578*, 3–30. (c) Benniston, A. C.; Gouille, V.; Harriman, A.; Lehn, J.-M.; Marczinke, B. *J. Phys. Chem.* **1994**, *98*, 7798–7804. (d) Lehn, J.-M. In *Nonlinear Optical Properties of Organic Molecules and Crystals*; Chemla, D. S., Zyss, J., Eds.; Academic Press: Orlando, FL, 1987; Vol. *2*, Chapter IV-1.
(7) (a) Ziessel, R.; De Nicola, A. *C. R. Chim.* **2009**, *12*, 450–478. (b) Harriman, A.; Ziessel, R. *Faraday Discuss.* **2006**, *131*, 377–391. (c) Cotton, F. A.; Chao, H.; Li, Z.; Murillo, C. A.; Wang, Q. *J. Organomet. Chem.* **2008**, *693*, 1412–1419. (d) Dong, T.-Y.; Lin, H.-Y.; Lin, S.-F.; Huang, C.-C.; Wen, Y.-S.; Lee, L. *Organometallics* **2008**, *27*, 555–562. (e) Barigelletti, F.; Flamigni, L. *Chem. Soc. Rev.* **2000**, *29*, 1–12. (f) Ward, M. D. *Chem. Soc. Rev.* **1995**, *24*, 121–134.
(8) (a) Demas, J. N.; DeGraff, B. A. *Coord. Chem. Rev.* **2001**, *211*, 317–351. (b) Fabbrizzi, L.; Licchelli, M.; Rabaioli, G.; Taglietti, A. *Coord. Chem. Rev.* **2000**, *205*, 85–108. (c) Keefe, M. H.; Benkstein, K. D.; Hupp, J. T. *Coord. Chem. Rev.* **2000**, *205*, 201–228. (d) Woessner, S. M.; Helms, J. B.; Houlis, J. F.; Sullivan, B. P. *Inorg. Chem.* **1999**, *38*, 4380–4381. (e) Demas, J. N.; DeGraff, B. A. *J. Chem. Educ.* **1997**, *74*, 690–695. (f) Slone, R. V.; Hupp, J. T.; Stern, C. L.; Albrecht-Schmitt, T. E. *Inorg. Chem.* **1996**, *35*, 4096–4097. (g) Klimant, I.; Wolfbeis, O. S. *Anal. Chem.* **1995**, *67*, 3160–3166. (h) Demas, J. N.; DeGraff, B. A. *Anal. Chem.* **1991**, *63*, 829A–837A.

Published on Web 03/25/2010

In order to effectively utilize transition-metal complexes in the above applications, the scope and limitations of excited-state reagents must be defined through the characterization of many complexes. The approach most often taken involves the synthesis of a series of compounds in a specific metal oxidation state with variations in the electronic properties of the coordinating ligands. Spectroscopic methods are then used to probe the microphysical changes produced in the photophysical properties, allowing molecules to be designed with specific properties and purposes. This approach is directly dependent on the ability to synthesize and isolate a complex in the desired oxidation state. In our laboratory, we have hypothesized that many luminescent transition-metal complexes may exist in electron configurations other than the common examples known in the literature (e.g., d^6, d^8, or d^{10}) and may not always be synthetically accessible. Therefore, by using spectroelectrochemical techniques to complement new synthetic strategies, the spectral properties of a reversible metal redox couple rather than a specific oxidation state can be investigated.

With this strategy, we discovered that the in situ electrogenerated Re^{II} complex $[Re(dmpe)_3]^{2+}$, where dmpe is 1,2-bis(dimethylphosphino)ethane, is emissive in a room temperature acetonitrile solution with a quantum efficiency (Φ) of 0.066,[9] which is 50% greater than the metal-to-ligand charge-transfer (MLCT) emission from $[Ru(bpy)_3]^{2+}$ ($\Phi = 0.042$).[10] $[Re(dmpe)_3]^{+}$ undergoes a one-electron reversible oxidation to $[Re(dmpe)_3]^{2+}$. Upon oxidation, new absorption bands in the visible region of the spectrum are observed and are responsible for luminescence. The lowest-energy transition is assigned to a spin-allowed σ(P) to dπ(Re) ligand-to-metal charge-transfer (LMCT) excited state ($\lambda_{max} = 530$ nm; $\varepsilon = 2110\ M^{-1}cm^{-1}$).[9] Recently reported unrestricted open-shell time-dependent density functional theory calculations for $[Re(dmpe)_3]^{2+}$ and the technetium analogue $[Tc(dmpe)_3]^{2+}$ support our initial assignment of the lowest-energy transition as a LMCT transition.[11]

Emission from $[Re(dmpe)_3]^{2+}$ is unique for several reasons. Luminescence from low-valent rhenium is dominated by rhenium(I) pyridyl/polypyridyl and carbonyl-based complexes,[12] although other examples of Re^{I} coordination complexes have exhibited photoactivity in solution.[13] $[Re(dmpe)_3]^{2+}$ appears to be a rare example of a d^5 transition-metal complex that exhibits room temperature luminescence in solution. Furthermore, it is one of only several examples of molecules with luminescence originating from a LMCT excited state in solution.[14] To the best of our knowledge, the only reported examples of luminescent d^5 molecules with LMCT excited states include $[Ru(CN)_6]^{3-}$ at 77 K[15] and $(\eta^5\text{-}C_5Me_5)_2Re$, which exhibits weak room temperature luminescence at 605 nm in toluene.[14r] Another important feature of $[Re(dmpe)_3]^{2+}$ is the highly oxidizing nature of the excited state. Del Negro et al. established through quenching studies with a series of substituted aromatic hydrocarbons that the excited-state potential, $E_{1/2}(Re^{2+*}/Re^{+})$, was +2.58 V vs SCE.[11]

In this manuscript, we have developed new synthetic strategies to obtain low-valent rhenium phosphine complexes with the general formula $[Re(dmpe)_{3-x}(depe)_x]^{2+/+}$ [depe = 1,2-bis(diethylphosphino)ethane and $x = 0-3$]. The intent is to expand the series of luminescent Re^{II} complexes and investigate the scope of the electrochemical, spectroscopic, and photophysical properties exhibited by phosphine-based Re^{II} complexes. Within this series of complexes, slight variations in the donor properties dictated the ultimate oxidation state of the final product. In either case, photophysical characterization of the d^5 Re^{II} electron configuration is possible either by conventional techniques or by electrogeneration in a luminescence spectroelectrochemical cell. Thus, synthetic strategies do not initially have to target a single oxidation state for successful characterization of their photophysical behavior. Given their unique spectral and excited-state properties, there is significant potential for low-valent rhenium phosphine complexes to be used as photocatalysts in energy conversion schemes or chemical processes.

Experimental Section

Materials. $[Re(benzil)(PPh_3)Cl_3]$,[16] $[Re(dmpe)_2Cl_2][PF_6]$,[17] and $[Re(depe)_2Cl_2][PF_6]$[17] were prepared according to literature methods. Ethylene glycol dimethyl ether (DME) was purchased as anhydrous grade from Aldrich and purged with argon prior to use. Dimethylacetamide (DMA), ferrocene, and $[Ru(bpy)_3Cl_2]\cdot 6H_2O$ were also obtained from Aldrich; ferrocene was sublimed prior to use. $TlPF_6$ was purchased from Alfa Aesar. The ligands dmpe and depe were purchased from Strem

(9) Lee, Y. F.; Kirchhoff, J. R. *J. Am. Chem. Soc.* **1994**, *116*, 3599–3600.
(10) Nakamaru, K. *Bull. Chem. Soc. Jpn.* **1982**, *55*, 2697–2705.
(11) Del Negro, A. S.; Seliskar, C. J.; Heineman, W. R.; Hightower, S. E.; Bryan, S. A.; Sullivan, B. P. *J. Am. Chem. Soc.* **2006**, *128*, 16494–16495.
(12) (a) Thorp-Greenwood, F. L.; Coogan, M. P.; Hallett, A. J.; Laye, R. H.; Pope, S. J. A. *J. Organomet. Chem.* **2009**, *694*, 1400–1406. (b) Li, M.-J.; Kwok, W.-M.; Lam, W. H.; Tao, C. H.; Yam, V. W. W.; Philips, D. L. *Organometallics* **2009**, *28*, 1620–1630. (c) Coleman, A.; Brennan, C.; Vos, J. G.; Pryce, M. T. *Coord. Chem. Rev.* **2008**, *252*, 2585–2595. (d) Patrocinio, O. T.; Iha, N. Y. M. *Inorg. Chem.* **2008**, *47*, 10851–10857. (e) Obata, M.; Kitamura, A.; Mori, A.; Kameyama, C.; Czaplewska, J. A.; Tanaka, R.; Kinoshita, I.; Kusumoto, T.; Hashimoto, H.; Harada, M.; Mikata, Y.; Funabiki, T.; Yano, S. *J. Chem. Soc., Dalton Trans.* **2008**, 3292–3300. (f) Baba, A. I.; Shaw, J. R.; Simon, J. A.; Thummel, R. P.; Schmehl, R. H. *Coord. Chem. Rev.* **1998**, *171*, 43–59. (g) Kalyanasundaram, K. *Photochemistry of Polypridine and Porphyrin Complexes*; Academic Press: New York, 1992. (h) Lees, A. J. *Chem. Rev.* **1987**, *87*, 711–743.
(13) (a) Fischer, M. J.; Jelliss, P. A.; Phifer, L. M.; Rath, N. P. *Inorg. Chim. Acta* **2005**, *358*, 1531–1544. (b) Fischer, M. J.; Jelliss, P. A.; Orlando, J. H.; Phifer, L. M.; Rath, N. P. *J. Lumin.* **2005**, *114*, 60–64. (c) Glezen, M. M.; Lees, A. J. *J. Am. Chem. Soc.* **1988**, *110*, 3892–3897. (d) Stacy, N. E.; Conner, K. A.; McMillin, D. R.; Walton, R. A. *Inorg. Chem.* **1986**, *25*, 3649–3652.
(14) To the best of our knowledge, the only examples of room temperature emission in a fluid solution from complexes with LMCT excited-state assignments are as follows: (a) Loukova, G. V.; Huhn, W.; Vasiliev, V. P.; Smirnov, V. A. *J. Phys. Chem. A* **2007**, *111*, 4117–4121. (b) Li, C.-K.; Cheng, E. C.-C.; Zhu, N.; Yam, V. W.-W. *Inorg. Chim. Acta* **2005**, *358*, 4191–4200. (c) Yam, V. W. W.; Lam, C. H.; Fung, W. K. M.; Cheung, K. K. *Inorg. Chem.* **2001**, *40*, 3435–3442. (d) Kunkely, H.; Vogler, A. *J. Photochem. Photobiol. A* **2001**, *146*, 63–66. (e) Williams, D. S.; Korolev, A. V. *Inorg. Chem.* **1998**, *37*, 3809–3819. (f) Yam, V. W. W.; Lo, K. K. W.; Wang, C. R.; Cheung, K. K. *J. Phys. Chem. A* **1997**, *101*, 4666–4672. (g) Yam, V. W. W.; Chan, C. L.; Cheung, K. K. *J. Chem. Soc., Dalton Trans.* **1996**, 4019–4022. (h) Yam, V. W. W.; Lo, K. K. W.; Cheung, K. K. *Inorg. Chem.* **1996**, *35*, 3459–3462. (i) Yam, V. W. W.; Lee, W. K.; Cheung, K. K.; Crystall, B.; Phillips, D. *J. Chem. Soc., Dalton Trans.* **1996**, 3283–3287. (j) Williams, D. S.; Thompson, D. W.; Korolev, A. V. *J. Am. Chem. Soc.* **1996**, *118*, 6526–6527. (k) Heinselman, K. S.; Hopkins, M. D. *J. Am. Chem. Soc.* **1995**, *117*, 12340–12341. (l) Pfennig, B. W.; Thompson, M. E.; Bocarsly, A. B. *Organometallics* **1993**, *12*, 649–655. (m) Yam, V. W. W.; Lee, W. K.; Lai, T. F. *J. Chem. Soc., Chem. Commun.* **1993**, 1571–1573. (n) Turk, T.; Resch, U.; Fox, M. A.; Vogler, A. *J. Phys. Chem.* **1992**, *96*, 3818–3822. (o) Paulson, S.; Sullivan, B. P.; Caspar, J. V. *J. Am. Chem. Soc.* **1992**, *114*, 6905–6906. (p) Sabin, F.; Ryu, C. K.; Ford, P. C.; Vogler, A. *Inorg. Chem.* **1992**, *31*, 1941–1945. (q) Kunkely, H.; Vogler, A. *J. Chem. Soc., Chem. Commun.* **1990**, 1204–1205. (r) Pfennig, B. W.; Thompson, M. E.; Bocarsly, A. B. *J. Am. Chem. Soc.* **1989**, *111*, 8947–8948. (s) Bandy, J. A.; Cloke, F. G. N.; Cooper, G.; Day, J. P.; Girling, R. B.; Graham, R. G.; Green, J. C.; Grinter, R.; Perutz, R. N. *J. Am. Chem. Soc.* **1988**, *110*, 5039–5050.
(15) Volger, A.; Kunkley, H. *Inorg. Chim. Acta* **1981**, *53*, L215–L216.
(16) Rouschias, G.; Wilkinson, G. *J. Chem. Soc. A* **1967**, 993–1000.
(17) Vanderheyden, J.-L.; Heeg, M. J.; Deutsch, E. *Inorg. Chem.* **1985**, *24*, 1666–1673.

Chemicals. Argon was received as industrial grade from AGA and scrubbed of oxygen and moisture via a silica-supported Cr^{III} tower. Acetonitrile, methanol, and dichloromethane were purchased from Fisher as HPLC grade and used as received except for acetonitrile, which was distilled over CaO_2 (Fisher, certified grade). Tetraethylammonium perchlorate (TEAP; GFS Chemicals, polarographic grade) was dried in vacuo at 60 °C for 12 h. Tetrabutylammonium hexafluorophosphate (TBAHFP; Aldrich) was recrystallized from absolute ethanol and dried under vacuum at 60 °C for 12 h. Ethanol was purchased from Pharmco (200 proof, ACS/USP) and used as received. Water was deionized to a resistivity greater than 17 MΩ·cm with a Barnstead B-Pure filtration unit. All other reagents were used as purchased unless otherwise specified.

Synthesis of $Re^{I/II}$ Complexes. Because of the sensitivity of dmpe and depe to oxidation, all synthetic reactions were carried out on a Schlenk line under an inert argon atmosphere using solvents deoxygenated by an argon purge unless otherwise noted.

[Re(dmpe)$_3$][PF$_6$]. [Re(benzil)(PPh$_3$)Cl$_3$] (0.496 g, 0.648 mmol) was suspended in DME (10 mL) in a 50 mL three-neck, round-bottomed flask. $TlPF_6$ (0.747 g, 2.14 mmol) was suspended in DME (3 mL) and added to the reaction vessel. In an argon-purged glovebag, dmpe (1 g, 7 mmol) was added to DME (3 mL). This solution was then transferred to the reaction mixture with a cannula. The purple mixture was refluxed for 15 h and cooled at room temperature over 3 h. White solids were filtered from the yellow solution and washed with DME (2 × 5 mL). The product was dissolved in DMA (150 mL) and filtered from insoluble TlCl. The DMA filtrate was added dropwise to a saturated aqueous solution of KPF_6 (75 mL) with stirring. The resulting white salt was filtered, washed with distilled water (3 × 5 mL), recrystallized from a minimum of methanol, washed with diethyl ether (2 × 2 mL), and dried under vacuum. Yield: 0.230 g (45.5%). Anal. Calcd for $C_{18}H_{48}F_6P_7Re$: C, 27.66; H, 6.19. Found: C, 27.79; H, 6.19. M^+_{calcd} 635.1711; M^+_{measd} 635.1696.

Zn/Hg Amalgam. Zinc (5 g, 30 mesh) was swirled in a 250 mL Erlenmeyer flask with HCl (100 mL, 1 M) for approximately 5 min. The HCl was decanted from the zinc, and a saturated aqueous solution of $HgCl_2$ (50 mL) was added. Upon swirling, the zinc was coated with a shiny layer of mercury. The solid was filtered from the solution and washed with diethyl ether (30 mL).

[Re(depe)$_3$][PF$_6$]$_2$. [Re(benzil)(PPh$_3$)Cl$_3$] (0.565 g, 0.739 mmol) and a Zn/Hg amalgam (5.1 g) were suspended in 13 mL of DME in a 50 mL three-neck, round-bottomed flask. $TlPF_6$ (0.852 g, 2.44 mmol) was suspended in DME (5 mL) and added to the reaction vessel. In an argon-purged glovebag, depe (1 g, 5 mmol) was added to DME (3 mL). This solution was then transferred to the reaction mixture with a cannula. The dark-brown mixture was stirred 40 min at room temperature, then refluxed for 12.5 h, and cooled at room temperature over 1.5 h. The black solids and amalgam were filtered from the brown solution and washed with DME (3 × 2 mL). The washes were then combined with the brown solution. A saturated aqueous solution of KPF_6 (10 mL) was added, followed by distilled water (50 mL). The resultant brown solid was filtered from the colorless solution. The soluble portions of the solid were dissolved in methylene chloride (50 mL) and filtered from the red product. The product was washed with methylene chloride (5 × 3 mL) and recrystallized by dissolving in a minimal amount of heated acetonitrile (~100 mL), followed by the addition of HPF_6 (3 mL) and H_2O_2 (30%, 3 mL) and subsequent slow cooling. Red crystals of the product were washed with diethyl ether (2 × 2 mL) and dried under vacuum. Yield: 0.038 g (4.7%). Anal. Calcd for $C_{30}H_{72}F_{12}P_8Re$: C, 32.98; H, 6.58; N, 0.00. Found: C, 33.51; H, 6.28; N, 0.04. M^+_{calcd} 803.3589; M^+_{measd} 803.3626.

[Re(dmpe)$_2$(depe)][PF$_6$]. [Re(dmpe)$_2$Cl$_2$][PF$_6$] (0.211 g, 0.300 mmol) was suspended in DME (5 mL) in a 50 mL three-neck, round-bottomed flask. $TlPF_6$ (0.349 g, 1.00 mmol) was suspended in DME (1.5 mL) and added to the reaction vessel. In an argon-purged glovebag, depe (0.31 g, 1.5 mmol) was added to DME (1.5 mL). This solution was then transferred to the reaction mixture with a cannula. The yellow reaction mixture was stirred for 1 h, refluxed for 12 h, and cooled to room temperature over 2 h to give a white powder. The white solid was filtered from the black solution and washed with DME (3 × 2 mL). The product was dissolved in acetonitrile (50 mL) and filtered from insoluble TlCl. The formation of single crystals suitable for X-ray analysis was achieved by concentration to 20 mL with heating, followed by the addition of 20 mL of hot distilled water and slow cooling to room temperature. Yield: 0.093 g (38.0%). Anal. Calcd for $C_{22}H_{56}F_6P_7Re$: C, 31.54; H, 6.74. Found: C, 31.66; H, 6.78. M^+_{calcd} 691.2338; M^+_{measd} 691.2349.

[Re(dmpe)$_2$(depe)][PF$_6$]$_2$. [Re(dmpe)$_2$(depe)][PF$_6$] (0.0342 g, 0.049 mmol) was dissolved in 1 mL of acetonitrile with stirring. Aqueous HPF_6 (0.5 mL) was added dropwise, producing a pink solution. The dropwise addition of 30% hydrogen peroxide (0.8 mL) resulted in the precipitation of [Re(dmpe)$_2$(depe)][PF$_6$]$_2$. The precipitate was then redissolved in acetonitrile (1 mL), followed by a second addition of HPF_6 (1 mL) and 30% hydrogen peroxide (1 mL). The solution was filtered, and the crude product was recrystallized in hot acetonitrile or 40% acetonitrile/water. Slow cooling produced X-ray-quality crystals.

[Re(dmpe)(depe)$_2$][PF$_6$]$_2$. [Re(depe)$_2$Cl$_2$][PF$_6$] (0.187 g, 0.229 mmol) and Zn/Hg amalgam (5.4 g) were suspended in DME (5 mL) in a 50 mL three-neck, round-bottomed flask. $TlPF_6$ (0.350 g, 1.00 mmol) was suspended in DME (1.5 mL) and added to the reaction vessel. In an argon-purged glovebag, dmpe (0.35 g, 2.3 mmol) was added to DME (1.5 mL). This solution was then transferred to the reaction mixture with a cannula. The yellow-green solution was stirred for 45 min at room temperature, refluxed for 12.5 h, and cooled to room temperature over 1.5 h. The gray solids and amalgam were filtered from the yellow solution and washed with DME (3 × 2 mL). The solid was further triturated with DME (3 × 1 mL), and all DME solutions were combined. The solution was held at room temperature for 3 h, during which time it became pink. A saturated aqueous solution of KPF_6 was added to the DME solution to precipitate the product. Recrystallization from warm acetonitrile (approximately 50 mL) with the addition of water (25 mL) afforded crystals of the red product, which were washed with diethyl ether (2 × 2 mL) and dried in vacuo. Yield: 0.163 g (68.0%). Anal. Calcd for $C_{26}H_{64}F_{12}P_8Re$: C, 30.06; H, 6.21. Found: C, 30.26; H, 6.54. M^+_{calcd} 747.2964; M^+_{measd} 747.2979.

Instrumentation and Methods. Mass Spectrometry. Mass spectra were recorded at the Mass Spectrometry and Proteomics Facility at The Ohio State University. An accurate mass determination for each of the four complexes was completed using a Waters Micromass LCT time-of-flight liquid chromatograph/electrospray mass spectrometer. All spectra were collected in acetonitrile.

Electrochemistry. Conventional electrochemical measurements were carried out in a specially designed Innovative Technologies, Inc., glovebox equipped with a sealed LEMO feedthrough connector [Bioanalytical Systems, Inc. (BAS), EW-7524] mounted in the back wall. This connector allowed facile connection to an external BAS 100B/W electrochemical analyzer and an internal cable to the electrochemical cell. A three-electrode configuration was utilized, consisting of a platinum working electrode (BAS model MF-2013), a platinum wire auxiliary electrode, and an acetonitrile-based $Ag/AgNO_3$ (0.01 M) reference electrode (BAS model MF-2062). Electrochemical data were collected in acetonitrile for 1 mM solutions of [Re(dmpe)$_3$][PF$_6$], [Re(dmpe)$_2$(depe)][PF$_6$], and [Re(dmpe)(depe)$_2$][PF$_6$]$_2$ with three different electrolyte systems: 0.1 M TBAHFP, 0.1 M TEAP, and 0.01 M TEAP. [Re(depe)$_3$][PF$_6$]$_2$ was only sufficiently soluble (1 mM) in 0.01 M TEAP. Ferrocene was also run in parallel in each electrolyte solution as an external reference standard. All potentials for the $Re^{III/II}$ and $Re^{II/I}$ redox couples from cyclic

voltammetry measurements are reported versus the ferrocene redox system.

Absorption Spectroelectrochemistry. Measurements were carried out with a gold optically transparent thin-layer electrode (OTTLE) as the working electrode.[18] The only modification to the reported cell design was the use of Varian Torr Resin Sealant instead of epoxy due to solubility differences in acetonitrile. A Varian Cary 5 UV−vis−NIR spectrophotometer in dual-beam mode was used for all measurements. An OTTLE cell, identical to the working electrode and filled with acetonitrile, was used in the spectrophotometer reference compartment. Potentials were controlled with a BAS CV-27 potentiostat and monitored with a Keithley model 197A digital multimeter. An electrolysis time of 4 min at each potential step was found to be sufficient to attain equilibrium values for [O]/[R] for both $[Re(dmpe)_3][PF_6]$ and $[Re(dmpe)(depe)_2][PF_6]_2$. $[Re(dmpe)_2(depe)][PF_6]$ required a 5 min electrolysis time. The concentration of all samples was 1 mM in a 0.1 M TEAP/acetonitrile solution. $[Re(depe)_3][PF_6]_2$ was not sufficiently soluble to perform spectroelectrochemical measurements.

Luminescence Spectroscopy. Luminescence measurements were conducted with an Aminco-Bowman Series 2 (SLM Instruments, Inc.) spectrophotometer. Where required, a Corning glass filter no. 0-52 (Esco Products, Inc.) was used to eliminate lamp artifacts. Room temperature measurements were conducted for $[Re(dmpe)(depe)_2][PF_6]_2$ in acetonitrile at a concentration of 0.14 mM. $[Re(depe)_3][PF_6]_2$ was not sufficiently soluble to make a solution of known concentration; thus, studies were carried out on a saturated solution. A 2.8×10^{-6} M solution of $[Ru(bpy)_3Cl_2]\cdot 6H_2O$ in distilled, deionized water was used as the standard for determination of the quantum yield (Φ) for $[Re(dmpe)(depe)_2][PF_6]_2$.[10] Both the analyte and reference were absorbance matched and excited at 436 nm in order to simplify the analysis. All solutions were deoxygenated by three freeze−pump−thaw cycles prior to analysis. Luminescence measurements at 77 K were performed in a specially fashioned Dewar with a 1-cm-diameter quartz tip. The samples were dissolved in 4:1 ethanol/methanol and transferred to a standard NMR tube for freezing. The concentrations used for $[Re(dmpe)_3]^{2+}$ and $[Re(dmpe)(depe)_2]^{2+}$ were 1.9 and 0.15 mM, respectively.

A long-optical-path luminescence spectroelectrochemical cell[19,20] was used to examine luminescence of the Re^{II} form of $[Re(dmpe)_3][PF_6]$ and $[Re(dmpe)_2(depe)][PF_6]$. The Re^{II} complexes were generated by application of a potential step sufficient to quantitatively oxidize the Re^{I} form of the complex to Re^{II}. Spectra were recorded after controlled potential electrolysis for 25 min to completely generate the Re^{II} complexes. The quantum yield was determined by absorbance matching (0.04 au) the rhenium complex in acetonitrile and $[Ru(bpy)_3Cl_2]\cdot 6H_2O$ in distilled deionized water and exciting both at 417 nm. All solutions were deoxygenated for 15 min with argon.

X-ray Measurements. $[Re(dmpe)_2(depe)][PF_6]$ and $[Re(dmpe)_2(depe)][PF_6]_2$. Data for a colorless crystal of $[Re(dmpe)_2(depe)][PF_6]$ ($0.32 \times 0.28 \times 0.12$ mm) and a red crystal of $[Re(dmpe)_2(depe)][PF_6]_2$ ($0.1 \times 0.1 \times 0.04$ mm) were collected with a SMART Platform diffractometer equipped with graphite-monochromated Mo Kα radiation and a 1K CCD area detector. The intensity data were corrected for absorption using *SADABS*.[21] The structure was solved and refined using *SHELXTL*, version 5.10.[22]

While the crystal lattice of $[Re(dmpe)_2(depe)][PF_6]$ contains solely anions and cations in a 1:1 ratio, the solid-state structure of $[Re(dmpe)_2(depe)][PF_6]_2$ crystallized with an additional acetonitrile molecule in the lattice with a cation/anion/solvent ratio of 1:2:1. Both structures are severely disordered. In the crystal lattice of $[Re(dmpe)_2(depe)][PF_6]$, the cation shows a rare case of total molecular disorder, with the Λ and Δ isomers of $[Re(dmpe)_2(depe)]^+$ occupying the same crystallographic position in a ratio of 45:55. Additionally, each of the four in-plane fluorine atoms of the $[PF_6]^-$ counterion has been refined over two positions, with the other two fluorine atoms not being disordered. The severe disorder of the cation in the crystal structure of $[Re(dmpe)_2(depe)][PF_6]_2\cdot CH_3CN$ has been modeled with one phosphorus atom and all but four carbon atoms of the two dmpe ligands disordered over two positions. Furthermore, one of the two crystallographically independent $[PF_6]^-$ ions is best described as a set of three octahedra, while the model for the other $[PF_6]^-$ contains three positions for each of the four in-plane fluorine atoms. Thus, the final refinements included anisotropic atomic displacement factors for all atoms that were not disordered and isotropic atomic displacement factors for all other non-hydrogen atoms. The final full-matrix least-squares refinements included the hydrogen atoms as "riding" atoms on calculated positions and converged to R1 = 3.34% (F, observed data) and wR2 = 8.95% (F^2, all data) for $[Re(dmpe)_2(depe)][PF_6]$ and R1 = 5.59% (F, observed data) and wR2 = 13.84% (F^2, all data) for $[Re(dmpe)_2(depe)][PF_6]_2\cdot CH_3CN$. Further details of the refinements are given in Table 1.

Table 1. Crystallographic Data and Structure Refinement Parameters for $[Re(dmpe)_2(depe)][PF_6]$ and $[Re(dmpe)_2(depe)][PF_6]_2\cdot CH_3CN$

	$[Re(dmpe)_2(depe)][PF_6]$	$[Re(dmpe)_2(depe)][PF_6]_2\cdot CH_3CN$
formula	$C_{22}H_{56}F_6P_7Re$	$C_{24}H_{59}F_{12}NP_8Re$
fw, g mol^{-1}	837.66	1023.68
space group	$P2(1)/n$	$P\bar{1}$
a, Å	10.2719(10)	10.8891(9)
b, Å	21.078(2)	11.3233(9)
c, Å	15.7963(16)	19.400(3)
α, deg		73.211(7)
β, deg	100.194(2)	79.304(7)
γ, deg		64.972(3)
V, Å^3	3366.1(6)	2069.5(4)
Z	4	2
D_{calcd}, g cm^{-3}	1.653	1.643
T, K	294(2)	293(2)
λ, Å	0.71073	0.71073
μ, mm^{-1}	3.989	3.318
data/restraints/param	9094/0/298	9912/0/436
R1/wR2 [$I_0 > 2\sigma(I)$]	0.0334/0.0831	0.0559/0.1216
R1/wR2 (all data)	0.0458/0.0895	0.1001/0.1384

Results and Discussion

Synthesis and Characterization. The initial synthetic route to prepare $[Re(dmpe)_3]^+$ was reported by Deutsch et al.[23] and involved a two-step reduction−substitution procedure via high-temperature, high-pressure bomb reactions starting with $[ReO_4]^-$. Subsequently, an alternative route was developed that allowed the direct synthesis of $[Re(dmpe)_3]^+$ from either of the Re^{V} precursors $[ReO_2(Py)_4]^+$ or $[ReOCl_2(OEt)(PPh_3)_2]$ (Py = pyridine, Et = C_2H_5, Ph = C_6H_5), with excess dmpe and a thiophenol catalyst.[24] The latter approach eliminated the need for the bomb reactor and simplified the overall synthesis. Given the unique photophysical properties of $[Re(dmpe)_3]^+$ and the interest in potential medical applications of radiopharmaceutical analogues of technetium and rhenium,[25]

(18) DeAngelis, T. P.; Heineman, W. R. *J. Chem. Educ.* **1976**, *53*, 594–597.
(19) Lee, Y. F.; Kirchhoff, J. R. *Anal. Chem.* **1993**, *65*, 3430–3434.
(20) Kirchhoff, J. R. *Curr. Sep.* **1997**, *16:1*, 11–14.
(21) Sheldrick, G. M. *SADABS*; University of Göttingen: Göttingen, Germany, **1996**.
(22) Sheldrick, G. M. *Acta Crystallogr.* **2008**, *A64*, 112–122.
(23) Deutsch, E.; Libson, K.; Vanderheyden., J.-L.; Ketring, A. R.; Maxon, H. R. *Nucl. Med. Biol.* **1986**, *13*, 465–477.
(24) Chang, L.; Deutsch, E. *Inorg. Synth.* **1997**, *31*, 253–256.
(25) (a) Garcia, R.; Paulo, A.; Santos, I. *Inorg. Chim. Acta* **2009**, *362*, 4315–4327. (b) Ferro-Flores, G.; de Murphy, C. A. *Adv. Drug Delivery Rev.* **2008**, *60*, 1389–1401. (c) Santos, I.; Paulo, A.; Correis, J. D. G. *Top. Curr. Chem* **2005**, *252*, 45–84.

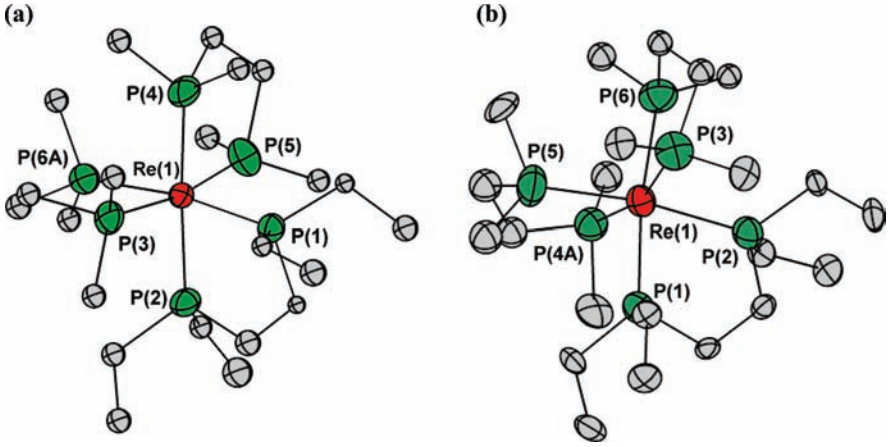

Figure 1. ORTEP diagrams of (a) $[Re(dmpe)_2(depe)]^+$ and (b) $[Re(dmpe)_2(depe)]^{2+}$ cations. Carbon atoms are shown as 20% probability ellipsoids, while the rhenium and phosphorus atoms are shown at 50%.

it is important to have facile procedures for the synthesis of low-valent rhenium complexes with phosphine-based ligands.

The synthetic approach developed in this work was motivated by the report by Helberg et al. for the synthesis of $[Re(bpy)_3][PF_6]_2$.[26] It was logically deduced that a similar synthesis of complexes of Re^I or Re^{II} with phosphine ligands would be highly successful because of the greater ability of phosphine ligands to stabilize low-valent rhenium relative to α,α′-diimine ligands. Thus, the synthesis of the homoleptic tris complexes $[Re(dmpe)_3]^+$ and $[Re(depe)_3]^+$ utilized the versatile Re^{III} starting material $[Re(benzil)(PPh_3)Cl_3]$, Tl^+ as a chloride ion scavenger, and dmpe or depe (in excess) as both the phosphine ligand and reductant. The synthesis with dmpe yielded the Re^I complex $[Re(dmpe)_3][PF_6]$ with an overall yield of 45.5%, which is acceptable compared to the previously published yields (cf. 70%[23] and ∼50%[24]). In contrast, when the phosphine was depe, a Zn/Hg amalgam was required to aid in the reduction of the rhenium and resulted in isolation of the Re^{II} complex $[Re(depe)_3][PF_6]_2$ with a yield of only 4.7%. The analogous bomb reaction was carried out for depe and resulted in a comparable yield of 4.5%.

The synthesis of new mixed-ligand phosphine complexes via the bomb reaction method results in a complicated mixture, which would require tedious separation steps and result in dramatically reduced yields. Following a strategy similar to that above, mixed-ligand complexes were readily prepared starting from $[Re(dmpe)_2Cl_2][PF_6]$ and $[Re(depe)_2Cl_2][PF_6]$ by the addition of an excess of the other phosphine. $[Re(dmpe)_2(depe)][PF_6]$ and $[Re(dmpe)(depe)_2][PF_6]_2$ were isolated as the Re^I and Re^{II} complexes, respectively. In the case of the bis(depe) complex, a Zn/Hg amalgam was used to assist reduction and was found to improve the yield in excess of 30%. For each of the complexes, the mass spectrum and elemental analysis confirmed their identity. Furthermore, the molecular ion peak in the mass spectra contained the characteristic signature of the rhenium 185 and 187 isotopes with an expected abundance ratio of approximately 2:3.

(26) Helberg, L. E.; Orth, S. D.; Sabat, M.; Harman, W. D. *Inorg. Chem.* **1996**, *35*, 5584–5594.

Table 2. Selected Bond Lengths (Å) and Angles (deg) for $[Re(dmpe)_2(depe)][PF_6]$ and $[Re(dmpe)_2(depe)][PF_6]_2\cdot CH_3CN$

$[Re(dmpe)_2(depe)][PF_6]$		$[Re(dmpe)_2(depe)][PF_6]_2\cdot CH_3CN$	
Re(1)−P(1)	2.4027(10)	Re(1)−P(1)	2.467(2)
Re(1)−P(2)	2.4078(11)	Re(1)−P(2)	2.4676(19)
Re(1)−P(3)	2.3875(11)	Re(1)−P(3)	2.460(2)
Re(1)−P(4)	2.3878(12)	Re(1)−P(4A)	2.422(5)
Re(1)−P(5)	2.3816(11)	Re(1)−P(4B)	2.481(6)
Re(1)−P(6A)	2.414(2)	Re(1)−P(5)	2.445(2)
Re(1)−P(6B)	2.367(3)	Re(1)−P(6)	2.451(2)
P(1)−Re(1)−P(2)	81.29(4)	P(1)−Re(1)−P(2)	80.93(6)
P(3)−Re(1)−P(6A)	79.73(6)	P(4A)−Re(1)−P(5)	77.98(15)
P(5)−Re(1)−P(4)	85.69(5)	P(5)−Re(1)−P(4B)	84.98(15)
P(6B)−Re(1)−P(5)	79.17(8)	P(6)−Re(1)−P(3)	80.94(8)
P(3)−Re(1)−P(4)	86.92(5)		
P(1)−Re(1)−P(6A)	170.78(6)	P(3)−Re(1)−P(4B)	173.17(15)
P(4)−Re(1)−P(2)	175.36(4)	P(4A)−Re(1)−P(3)	163.96(15)
P(5)−Re(1)−P(3)	170.53(5)	P(5)−Re(1)−P(2)	171.60(7)
P(6B)−Re(1)−P(1)	168.25(7)	P(6)−Re(1)−P(1)	172.51(7)
P(2)−Re(1)−P(6A)	91.39(6)	P(1)−Re(1)−P(4B)	90.10(15)
P(3)−Re(1)−P(1)	94.98(4)	P(2)−Re(1)−P(4B)	91.95(14)
P(3)−Re(1)−P(2)	93.09(5)	P(3)−Re(1)−P(1)	96.11(7)
P(4)−Re(1)−P(1)	94.08(4)	P(3)−Re(1)−P(2)	91.84(7)
P(4)−Re(1)−P(6A)	93.17(6)	P(4A)−Re(1)−P(1)	96.61(14)
P(5)−Re(1)−P(1)	91.45(4)	P(4A)−Re(1)−P(2)	99.78(14)
P(5)−Re(1)−P(2)	94.76(5)	P(4A)−Re(1)−P(6)	87.54(14)
P(5)−Re(1)−P(6A)	94.77(6)	P(5)−Re(1)−P(1)	91.25(8)
P(6B)−Re(1)−P(2)	92.37(7)	P(5)−Re(1)−P(3)	92.02(8)
P(6B)−Re(1)−P(3)	95.23(8)	P(5)−Re(1)−P(6)	95.73(8)
P(6B)−Re(1)−P(4)	92.25(8)	P(6)−Re(1)−P(2)	92.24(7)
P(3)−Re(1)−P(4)	86.92(5)	P(6)−Re(1)−P(4B)	93.23(15)

Structural Characterization of $[Re(dmpe)_2(depe)][PF_6]$ and $[Re(dmpe)_2(depe)][PF_6]_2\cdot CH_3CN$. ORTEP diagrams of $[Re(dmpe)_2(depe)]^+$ and $[Re(dmpe)_2(depe)]^{2+}$ are shown in Figure 1. Table 1 summarizes the crystallographic data and structural refinement parameters for the crystal structures of both complexes, while Table 2 presents selected bond lengths and angles.

The local coordination geometry around the rhenium metal center is characterized as a distorted octahedron with six Re−P bonds in both structures. The average Re−P bond lengths for the Re^I and Re^{II} complexes are 2.393 ± 0.016 and 2.456 ± 0.019 Å, respectively. The shorter length of the Re^I−P bond relative to that of the Re^{II} complex is likely a result of the higher degree of π-back-bonding in the more electron-rich Re^I form. This result is consistent with prior

EXAFS results for Re−P bond distances in $[Re(dmpe)_3]^+$ [2.387(10) Å] and $[Re(dmpe)_3]^{2+}$ [2.441(10) Å].[27] The means of the comparative bond angles about the metal centers are similar for both structures. The average diphosphine P−Re−P bite angles for $[Re(dmpe)_2(depe)]^+$ and $[Re(dmpe)_2(depe)]^{2+}$ are 82.56° ± 3.53 and 81.21° ± 2.88, respectively. The average *trans*-phosphine angles are 171.23° ± 2.98 and 170.31° ± 4.28, while the average *cis*-phosphine angles are 92.87° ± 2.32 and 93.20° ± 3.32.

Related structures with the $Re-P_6$ core are scarce in the literature. The structure of $[Re(dppm)_3]^+$, where dppm is 1,2-bis(diphenylphosphino)methane, was reported as both the perrhenate[28] and iodide[29] salts and had Re−P bond lengths ranging from 2.408(3) to 2.473(3) Å and from 2.400(2) to 2.467(2) Å, respectively. By comparison, these are slightly longer than those observed for $[Re(dmpe)_2(depe)]^+$. The average P−Re−P bite angles (69.16° ± 0.91 and 68.66° ± 0.57) are significantly smaller owing to the shorter methylene bridge between the chelating phosphorus atoms. The closely related manganese analogue $[Mn(dmpe)_3]^+$ exhibits a highly symmetrical $Mn-P_6$ core and crystallizes in space group $P\bar{3}1c$.[30] The Mn−P bond distances are on average 0.1 Å shorter than those for $[Re(dmpe)_2(depe)]^+$, while the comparable angles are essentially the same. Zero-valent complexes of the type $[M(dmpe)_3]$, where M = Cr, Mo, W, V, Nb, and Ta, are also known.[31] These tris(dmpe) complexes were assigned to the cubic space group *Im*3*m*, showing a roughly octahedral orientation of the $M-P_6$ core.

The structural refinements for $[Re(dmpe)_2(depe)][PF_6]$ and $[Re(dmpe)_2(depe)][PF_6]_2\cdot CH_3CN$ showed good agreement between the data and the models [R1, $I > 2\sigma(I)$ = 3.34% for Re^I and 5.59% for Re^{II}]. Both models revealed a high degree of disorder within the crystals. $[Re(dmpe)_2(depe)][PF_6]$ was found to contain two propeller-like isomeric forms of the cation disordered over the same crystallographic position and disordered $[PF_6]^-$ moieties. The Λ and Δ isomers of the complex are shown in Figure 2 without the nonbridging carbon atoms. Space-filling models of each isomer illustrated the globular nature of both isomers. The similarity of the electron distribution on the surface of the molecules results in the possibility of cocrystallization of the two isomers. Unlike the analogous Re^I complex, $[Re(dmpe)_2(depe)][PF_6]_2\cdot CH_3CN$ crystallized with only one isomer present in the crystal, with two counterions for every cation occupying spaces formed in the gaps of the propellers of the complex.

Electrochemical Characterization. Table 3 summarizes the electrochemical data obtained from cyclic voltammetry studies in an acetonitrile solution. Three different supporting electrolyte solutions were examined for comparative purposes: 0.1 M TBAHFP, 0.1 M TEAP, and 0.01 M TEAP. $[Re(depe)_3]^{2+}$ was not soluble to a great enough degree in a 0.1 M solution of either TBAHFP or TEAP. Thus, a third study with 0.01 M TEAP was completed in order to obtain quantifiable results for this complex in comparison to the other complexes.

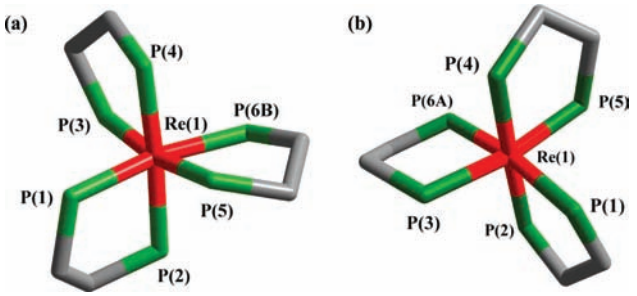

Figure 2. Wire diagrams of the (a) Λ and (b) Δ propeller-like isomers of $[Re(dmpe)_2(depe)]^+$, which are both present in the crystal lattice. Nonbridging carbon atoms have been removed to simplify the models.

Table 3. Summary of the Electrochemical and Spectroelectrochemical Redox Data for the $[Re(dmpe)_{3-x}(depe)_x]^{2+/+}$ (x = 0−3) Complexes

	$E^{o\prime}$,[a,b] V	$E^{o\prime}$,[a,c] V	$E^{o\prime}$,[a,d] V	$E^{o\prime}$,[e] V	n[e]
			$Re^{II/I}$		
$[Re(dmpe)_3]^+$	−0.11	−0.11	−0.09	−0.02	1.02
$[Re(dmpe)_2(depe)]^+$	−0.16	−0.16	−0.15	−0.08	0.96
$[Re(dmpe)(depe)_2]^{2+}$	−0.23	−0.23	−0.22	−0.14	1.19
$[Re(depe)_3]^{2+}$	*f*	*f*	−0.28	*f*	*f*
			$Re^{III/II}$		
$[Re(dmpe)_3]^+$	+0.78	+0.77	+0.80		
$[Re(dmpe)_2(depe)]^+$	+0.75	+0.73	+0.76		
$[Re(dmpe)(depe)_2]^{2+}$	+0.71	+0.69	+0.72		
$[Re(depe)_3]^{2+}$	*f*	*f*	+0.68		

[a] $E^{o\prime} = (E_{p,a} + E_{p,c})/2$ from cyclic voltammetry at 100 mV s^{-1} in acetonitrile solutions. Concentrations were 1 mM for all complexes except $[Re(depe)_3]^{2+}$. Potentials were determined versus $Ag/AgNO_3$ (0.01 M) nonaqueous (acetonitrile) reference electrode and are reported as volts versus a ferrocene external standard. [b] In 0.1 M TBAHFP. [c] In 0.1 M TEAP. [d] In 0.01 M TEAP. [e] Spectropotentiostatic determination in 0.1 M TEAP/acetonitrile. The potential was reported versus $Ag/AgNO_3$ (0.01 M) nonaqueous (acetonitrile) reference electrode. n is the number of electrons transferred. [f] Not determined because of the low solubility in this medium.

The voltammetric behavior for the $[Re(dmpe)_{3-x}(depe)_x]^{2+/+}$ complexes is the same in all three solvent−supporting electrolyte solutions. The voltammograms for $[Re(dmpe)_2(depe)]^+$ and $[Re(dmpe)(depe)_2]^{2+}$ in 0.1 M TBAHFP/acetonitrile are representative of the group and will be described in detail. Figure 3 depicts the cyclic voltammetric results for $[Re(dmpe)_2(depe)]^+$ at 100 mV s^{-1}. A scan initiated at −1.00 V in the positive direction exhibits two oxidation peaks at −0.13 and +0.82 V. Upon reversal of the scan, the corresponding reduction waves were observed at +0.69 and −0.20 V, with the reduction peak currents (i_{pc}) smaller in magnitude than the oxidation peak currents (i_{pa}). When the scan limits are confined to −0.60 to +0.40 V, the ratio of the peak currents (i_{pc}/i_{pa}) for the first redox couple ($E^{o\prime}$ = −0.16) is essentially unity (1.01). The peak currents for this redox couple are linearly proportional to the square root of the scan rate as defined by the Randles−Sevcik equation, $E^{o\prime}$ is independent of the scan rate, and the peak-to-peak separation (ΔE_p)

(27) Libson, K.; Woods, M.; Sullivan, J. C.; Watkins, J. W., II; Elder, R. C.; Deutsch, E. *Inorg. Chem.* **1988**, *27*, 999–1003.
(28) Whitmire, K. H.; Derringer, D. R.; Kongkasuwan, K. R. *Acta Crystallogr.* **2002**, *E58*, m363–m365.
(29) Rivero, M.; Kremer, C.; Gancheff, J.; Kremer, E.; Suescun, L.; Mombru, A.; Mariezcurrena, R.; Dominguez, S.; Mederos, A.; Midollini, S. *Polyhedron* **2000**, *19*, 2249–2254.
(30) Toupadakis, A.; Scott, B. L.; Kubas, G. J. *J. Chem. Crystallogr.* **2004**, *34*, 245–248.
(31) (a) Cloke, F. G. N.; Fyne, P. J.; Green, M. L. H.; Ledoux, M. J. *J. Organomet. Chem.* **1980**, *198*, C69–C71. (b) Cloke, F. G. N.; Fyne, P. J.; Gibson, V. C.; Green, M. L. H.; Ledoux, M. J.; Perutz, R. *J. Organomet. Chem.* **1984**, *277*, 61–73.

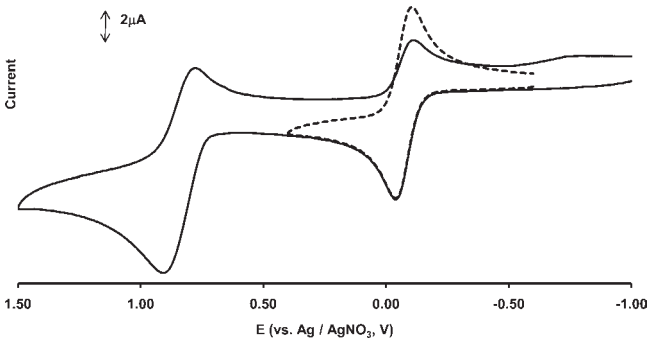

Figure 3. Cyclic voltammograms of 1 mM $[Re(dmpe)_2(depe)]^+$ in 0.1 M TBAHFP/acetonitrile at a platinum disk electrode: (- - -) positive potential scan between an initial/final potential of −0.60 V with a switching potential of +0.40 V; (—) positive potential scan between an initial/final potential of −1.00 V with a switching potential of +1.50 V. The scan rate is 100 mV s^{-1}.

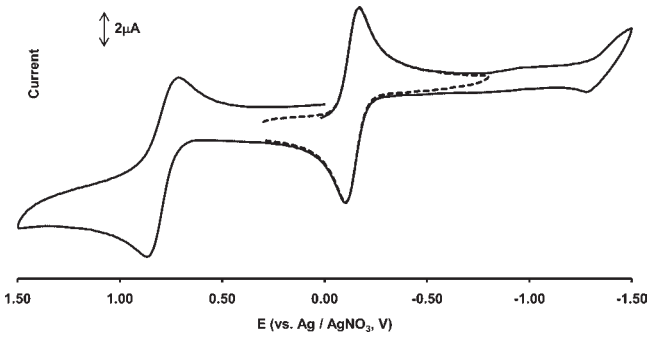

Figure 4. Cyclic voltammograms of 1 mM $[Re(dmpe)(depe)_2]^{2+}$ in 0.1 M TBAHFP/acetonitrile at a platinum disk electrode: (---) negative potential scan between an initial/final potential of +0.40 V with a switching potential of −0.80 V; (—) negative potential scan between an initial/final potential of +0.02 V with switching potentials of ±1.50 V. The scan rate is 100 mV s^{-1}.

is 66 mV for Figure 3, which for inorganic systems is in reasonable agreement with the value of 59 mV for a one-electron reversible couple, as predicted by the Nernst equation. On the basis of these observations, the first redox couple was found to be reversible by all standard Nernstian criteria[32] and is assigned to the one-electron oxidation of Re^{I} to Re^{II}. The second oxidation wave is assigned as the oxidation of the electrogenerated Re^{II} complex to Re^{III}. When the potential is cycled between −1.00 and +1.50 V, i_{pc}/i_{pa} values for the $Re^{II/I}$ and $Re^{III/II}$ redox couples are significantly less than 1. This indicates that oxidation to Re^{III} is irreversible and results in a loss of the electroactive species for the reverse scan from +1.50 to −1.00 V.

The cyclic voltammograms for $[Re(dmpe)(depe)_2]^{2+}$ are shown in Figure 4. In this case, the scan was initiated at +0.02 V in the negative potential direction and resulted in the one-electron reduction of Re^{II} to Re^{I} at −0.26 V. After the potential was switched at −1.50 V, the reoxidation to Re^{II} was observed at −0.19 V, completing the one-electron reversible electron transfer with i_{pc}/i_{pa} equal to 1.03 and peak currents proportional to the square root of the scan rate. As was the case with $[Re(dmpe)_2(depe)]^+$, oxidation to Re^{III} was observed at +0.78 V, followed by the reduction back to Re^{II} at +0.62 V on the reverse scan

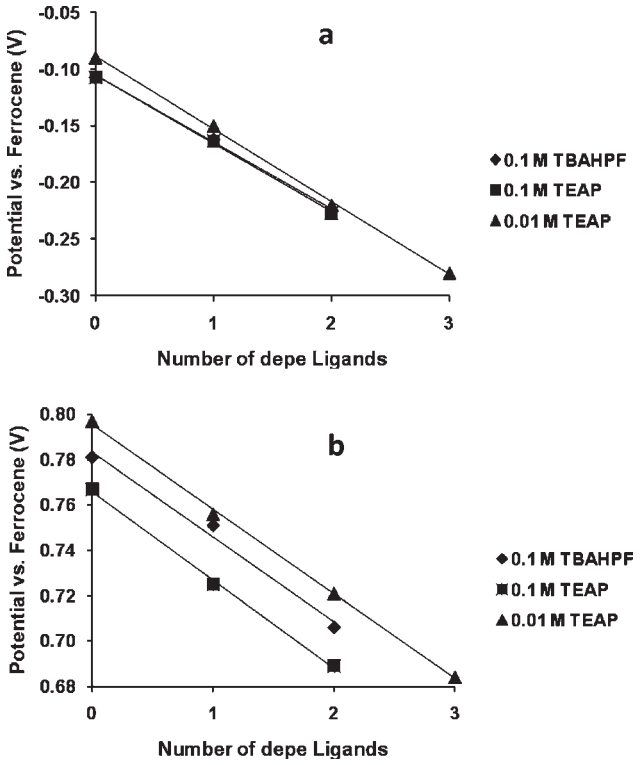

Figure 5. Plot of $E^{\circ\prime}$ (vs ferrocene external standard) from cyclic voltammetry for the (a) $Re^{II/I}$ and (b) $Re^{III/II}$ redox couples versus the number of depe ligands in each complex. The 0.1 M TBAHPF and 0.1 M TEAP lines in part a are essentially superimposed.

with i_{pc} reduced relative to i_{pa}. This reveals a loss of reversibility similar to that of $[Re(dmpe)_2(depe)]^+$. The voltammetric behavior for both mixed-ligand complexes is consistent with that previously reported for $[Re(dmpe)_3]^+$, which was attributed to decomposition of the Re^{III}-generated species, leading to some degree of chemical irreversibility.[33]

Figure 5 shows plots of the redox potentials of the $Re^{II/I}$ and $Re^{III/II}$ redox couples as a function of the number of depe ligands. A clear trend is established, regardless of the solvent and supporting electrolyte system, that indicates that the potentials for the $Re^{II/I}$ and $Re^{III/II}$ couples shift in a linear fashion to more negative potentials as the number of bound depe ligands is increased. This can be rationalized by the slightly greater σ-donor ability of having ethyl rather than methyl substituents on the phosphine ligands. In effect, as the weaker π acid ligand is added, the metal center is more easily oxidized, as signified by a more negative potential for the redox couple.[34] This result is also consistent with the synthetic results; i.e., the syntheses of the bis(depe) and tris(depe) compounds favor the formation of Re^{II} complexes whereas syntheses of the bis(dmpe) and tris(dmpe) compounds yield Re^{I} complexes. Furthermore, the addition of a Zn/Hg amalgam was beneficial to aiding in the reduction and achieving higher yields of the bis(depe) and tris(depe) Re^{II} complexes.

(32) *Laboratory Techniques in Electroanalytical Chemistry*; Kissinger, P. T., Heineman, W. R., Eds.; Marcel Dekker: New York, 1984.

(33) Kirchhoff, J. R.; Allen, M. R.; Cheesman, B. V.; Okamoto, K.-I.; Heineman, W. R.; Deutsch, E. *Inorg. Chim. Acta* **1997**, *262*, 195–202.

(34) Kirchhoff, J. R.; Heineman, W. R.; Deutsch, E. *Inorg. Chem.* **1987**, *26*, 3108–3113.

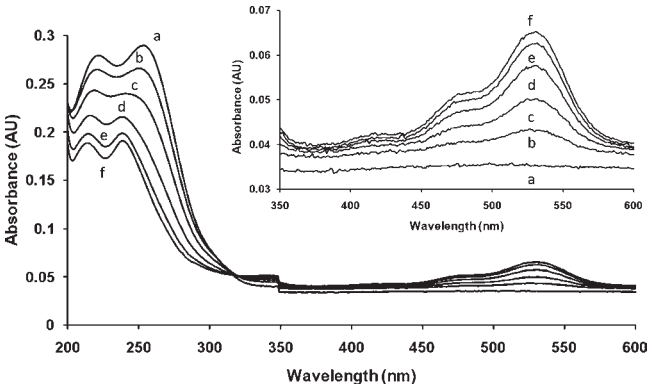

Figure 6. Sequential absorption spectra from 200 to 600 nm obtained during the spectropotentiostatic oxidation of 1 mM $[Re(dmpe)_2(depe)]^+$ in 0.1 M TEAP/acetonitrile. Applied potentials in V vs $Ag/AgNO_3$ are as follows: (a) −0.20; (b) −0.11; (c) −0.08; (d) −0.05; (e) −0.02; (f) +0.01. Inset: Expanded view of the visible absorption features from 350 to 600 nm.

Table 4. Summary of the Absorption Properties for the $[Re(dmpe)_{3-x}(depe)_x]^{2+/+}$ (x = 0−3) Complexes[a]

	λ_{max}, nm		
	Re^I	Re^{II}	λ_{iso}, nm
$[Re(dmpe)_3]^{2+/+}$	221, 252	528	320
$[Re(dmpe)_2(depe)]^{2+/+}$	222, 254	525	320
$[Re(dmpe)(depe)_2]^{2+/+}$	219, 252	530	330, 355
$[Re(depe)_3]^{2+/+}$	*b*	533	*b*

[a] Determined by spectroelectrochemical measurements in 0.1 M TEAP/acetonitrile. [b] Not determined because of low solubility.

Absorption Spectroelectrochemistry. Absorption spectroelectrochemistry is a very useful technique to characterize the reversible $Re^{II/I}$ redox couple of the $[Re(dmpe)_{3-x}(depe)_x]^{2+/+}$ complexes because either oxidation state can be isolated depending on the targeted ligand set. When the Re^I form is obtained, the isolated complexes are colorless in comparison to the red color of the Re^{II} form. Spectroelectrochemistry was also valuable to determine the stability of the two oxidation states and the absence of any other rhenium species in solution.

Figure 6 depicts the spectropotentiostatic oxidation of 1 mM $[Re(dmpe)_2(depe)]^+$ in 0.1 M TEAP/acetonitrile, which serves as a representative example for all of the $[Re(dmpe)_{3-x}(depe)_x]^{2+/+}$ complexes. In this experiment, the potential was gradually stepped from −0.20 to +0.01 V to illustrate the spectral changes during the conversion of the fully reduced form to the fully oxidized form, i.e., Re^I to Re^{II}. The spectrum of the Re^{II} species exhibits an absorption maximum at 525 nm (spectrum F), while the colorless Re^I species has absorption maxima at 222 and 254 nm. A clear isosbestic point is observed at 320 nm, indicating clean interconversion between the two redox states. A Nernst plot, E_{app} vs log([O]/[R]), is linear and yields $E^{o\prime} = -0.082$ V and $n = 0.96$, confirming a one-electron-transfer process.

Absorption spectroelectrochemical data for all four complexes are summarized in Tables 3 and 4 and are consistent with the absorption behavior previously reported for $[Re(dmpe)_3]^+$.[9] The electrochemical data are also internally consistent with the results from the cyclic voltammetry experiments in 0.1 M TEAP/acetonitrile vs the $Ag/AgNO_3$ (0.01 M) pseudo reference electrode. Table 4 shows that the absorption maxima for Re^I and Re^{II} species do not vary to a measurable degree with the change in the ligand system. Larger variations in the electronic properties of the ligand would likely result in more dramatic changes in the absorption spectrum.

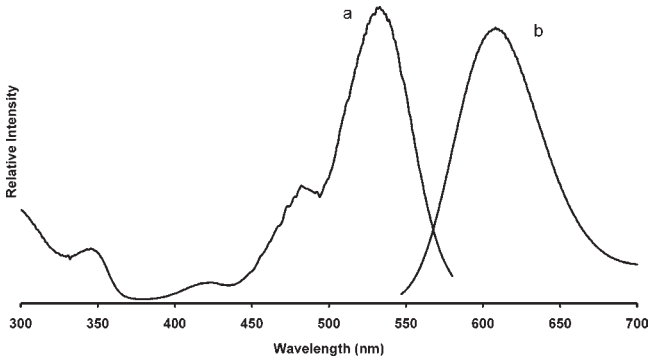

Figure 7. Corrected (a) excitation (λ_{em} = 600 nm; bandpass, 4 nm; PMT, 780 V) and (b) emission (λ_{ex} = 530 nm; bandpass, 4 nm; PMT, 700 V) spectra of 0.13 mM $[Re(dmpe)(depe)_2]^{2+}$ in acetonitrile at room temperature. Excitation spectrum obtained with a Corning no. 0-52 glass filter placed between the sample and emission monochromator.

Table 5. Summary of the Emission Properties for the $[Re(dmpe)_{3-x}(depe)_x]^{2+}$ (x = 0−3) Complexes

	λ_{max},[a] nm	Φ	λ_{max},[b] nm
$[Re(dmpe)_3]^{2+}$	604[c]	0.076	594
$[Re(dmpe)_2(depe)]^{2+}$	608[c]	0.067	*d*
$[Re(dmpe)(depe)_2]^{2+}$	608	0.066	602
$[Re(depe)_3]^{2+}$	610	*e*	*e*

[a] Corrected emission maximum at room temperature in deoxygenated acetonitrile. [b] Corrected emission maximum at 77 K in deoxygenated 4:1 ethanol/methanol. [c] Corrected emission maximum after spectropotentiostatic oxidation in 0.1 M TEAP/acetonitrile. [d] Re^{II} was only generated in situ in the spectroelectrochemical cell. [e] Compound not sufficiently soluble for accurate determination.

Luminescence. The excited-state properties of $[Re(dmpe)_3]^{2+}$ were previously investigated in detail.[9,11] The lowest-energy absorption band, which is responsible for the luminescence, was described as a spin-allowed doublet−doublet LMCT transition from σ(P) to dπ(Re). This conclusion was based on the relatively high molar absorptivity for the absorption at 530 nm (ε = 2110 M^{-1} cm^{-1}), a radiative rate constant of 10^6 s^{-1}, and an emission that was independent of the excitation wavelength. The emission from the newly synthesized $[Re(dmpe)_{3-x}(depe)_x]^{2+/+}$ complexes is attributed to the same type of LMCT state.

Steady-state excitation and emission measurements were obtained in an acetonitrile solution for the Re^{II} complexes $[Re(dmpe)(depe)_2]^{2+}$ and $[Re(depe)_3]^{2+}$. $[Re(dmpe)_3]^{2+}$ and $[Re(dmpe)_2(depe)]^{2+}$ were generated in situ and the emission properties measured with a luminescence spectroelectrochemical cell. Figure 7 shows the corrected excitation and emission spectra of $[Re(dmpe)(depe)_2]^{2+}$, which are typical for all of the complexes. The emission properties for the entire $[Re(dmpe)_{3-x}(depe)_x]^{2+/+}$ series are summarized in Table 5. As was previously observed for $[Re(dmpe)_3]^{2+}$,[9] the emission maximum for all complexes was independent of the excitation wavelength, with the intensity directly dependent on the

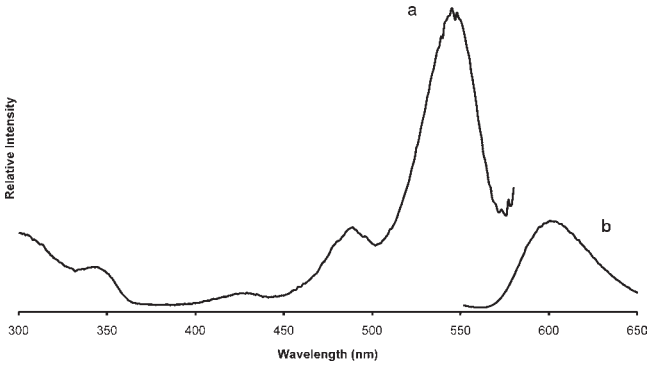

Figure 8. Corrected (a) excitation (λ_{em} = 600 nm; bandpass, 4 nm; PMT, 750 V) and (b) emission (λ_{ex} = 528 nm; bandpass, 4 nm; PMT, 700 V) spectra of 0.15 mM $[Re(dmpe)(depe)_2]^{2+}$ in 4:1 ethanol:methanol at 77 K. Excitation spectrum obtained with a Corning 0−52 glass filter placed between the sample and emission monochromator.

molar absorptivity at the exciting wavelength, indicating that emission occurs solely from the lowest excited state (530 nm). The quantum efficiency of the emission of $[Re(dmpe)(depe)_2]^{2+}$ in Figure 7 was determined to be 0.066. The quantum efficiencies are essentially the same for all complexes and consistent with the previously reported value for $[Re(dmpe)_3]^{2+}$ generated in situ in the luminescence spectroelectrochemical cell.[9] Φ for $[Re(depe)_3]^{2+}$ could not be accurately determined because of the low solubility of this complex in acetonitrile. The excitation spectrum for each complex paralleled its absorption spectrum.

The Re^{II} form of the tris(dmpe) complex was obtained by oxidation of the Re^{I} form with hydrogen peroxide and HPF_6. The emission of $[Re(dmpe)(depe)_2]^{2+}$ and $[Re(dmpe)_3]^{2+}$ was then measured at 77 K. Figure 8 shows the emission and excitation spectra of $[Re(dmpe)(depe)_2]^{2+}$ in a 4:1 ethanol/methanol glass. The spectra are similar to those obtained in the luminescence spectroelectrochemical study of $[Re(dmpe)_3]^{2+}$ and the steady-state luminescence spectra of $[Re(dmpe)(depe)_2]^{2+}$. The emission peak shows a small rigidochromic effect in both complexes; the emission maximum for $[Re(dmpe)_3]^{2+}$ changed from 604 nm in room temperature acetonitrile to 594 nm at 77 K, while the maximum for $[Re(dmpe)(depe)_2]^{2+}$ shifted from 608 nm in room temperature acetonitrile to 602 nm at 77 K. Excitation spectra for $[Re(dmpe)_3]^{2+}$ and $[Re(dmpe)(depe)_2]^{2+}$ at 77 K were very similar to those acquired in room temperature acetonitrile.

Conclusions

A new synthetic approach for the preparation of low-valent rhenium phosphine complexes with the general formula $[Re(dmpe)_{3-x}(depe)_x]^{2+/+}$ ($x = 0-3$) has been described, and the electrochemical and spectroscopic properties of the Re^{I} and Re^{II} oxidation states have been characterized. The final oxidation state is strongly influenced by the electron-donating properties of the phosphine ligand or ligand combination used in the synthesis. Stronger electron donors favored Re^{I} formation, while more π-acidic phosphine ligands favored Re^{II} formation. In each case, a reversible one-electron transfer is observed for the $Re^{II/I}$ redox couple, which permitted UV−vis and luminescence spectroelectrochemical characterization. Complexes in the Re^{II} oxidation state exhibit visible absorption bands from 350 to 600 nm, with the lowest-energy band assigned as a spin-allowed σ(P) to dπ(Re) LMCT transition. Excitation into the lowest-energy absorption band revealed rare examples of highly luminescent LMCT excited states from d^5 transition-metal complexes in a room temperature solution with $\Phi \approx 0.07$. Crystallographic characterization of $[Re(dmpe)_2(depe)]^{2+}$ and $[Re(dmpe)_2(depe)]^{+}$ provided important comparisons of the structural characteristics of both oxidation states.

Acknowledgment. Financial support from The University of Toledo is gratefully acknowledged. Funding for the Ohio Crystallography Consortium from the College of Arts and Sciences at The University of Toledo and the Ohio Board of Regents is also greatly appreciated. We also thank Professor A. Alan Pinkerton for helpful and interesting discussions with regards to the crystal structures.

Supporting Information Available: X-ray crystallographic data in CIF format. This material is available free of charge via the Internet at http://pubs.acs.org.